ELSEVIER

The importance of the equilibrium zincate ion concentration in modeling a cylindrical alkaline cell

J.J. Kriegsmann, H.Y. Cheh *

Department of Chemical Engineering and Applied Chemistry, Columbia University, 500 West, 120th street, New York, NY 10027 USA

Abstract

A mathematical model of the Zn/MnO_2 cylindrical alkaline cell is revised by using a more appropriate expression for the equilibrium zincate ion concentration. The new expression models the equilibrium behavior of solid zinc oxide in alkaline electrolyte, whereas the previous expression models the solid zinc dihydroxide equilibrium. The new expression results in the prediction of lower and more uniform zincate ion concentration profiles. The influence of the equilibrium zincate ion concentration is analyzed through the precipitation rate of zinc oxide. The zincate ion concentration profiles for the revised case are responsible for the simulated improvement in cell performance. Adverse cell voltage fluctuations near the end of discharging are determined to be caused by a localized region where the zincate ion concentration is zero. These fluctuations are considered numerical discrepancies and are not physically realistic. Numerical remedies that successfully remove the cell voltage fluctuations are provided, but they are employed by weakening the assumption of concentrated ternary electrolyte theory. © 1999 Elsevier Science S.A. All rights reserved.

Keywords: Alkaline batteries; Zincate ion; Precipitation rate; Discharge time

1. Introduction

The mathematical model presented by Podlaha and Cheh [1,2] for the Zn/MnO_2 cylindrical alkaline cell is considered well-developed. The model is being applied and revised before new phenomena are incorporated. These types of studies are important in the evaluation of the current model. Two optimization studies were performed in order to find best designs for an AA-size configuration by adjusting the initial cathode porosity [3] and the active material loading [4]. The results show that the model gives realistic predictions of the cell behavior when proper values of the influential parameters are used. Revision studies are necessary because certain aspects of the model lead to physically inconsistent predictions. For example, the cathode specific interfacial area was increased [5] in order to match the literature values more closely. The result was a much better prediction of the initial cell voltage for an AA-size design. However, nonphysical voltage fluctuations occurred because of a localized region with total zincate ion depletion.

This study considers the effect of the zincate ion concentration in greater detail. The incorporation of concentrated ternary electrolyte theory for this system creates many difficulties. For example, physical property data are lacking, and the physical influence of the zincate ion concentration on the cell performance is not completely known. When the zincate ion is totally consumed, the electrolyte should revert to a binary alkaline system without drastic polarization effects, but this transition is not easy to implement mathematically. Thus, the zincate ion concentration necessitates the revision of the ternary electrolyte properties, and it is also the cause of computational difficulties.

The first objective of this study is the removal of the incorrect modeling prediction of a large accumulation of zincate ion immediately after discharging starts. The analysis begins by revising the formulation used for the equilibrium zincate ion concentration. This quantity is important in quantifying the dissolution–precipitation mechanism used in describing the anode behavior of the Zn/MnO_2 system. The analysis of a single model parameter or correlation can give valuable information regarding the predictive capabilities of a battery model [5–7]. Using different formulations for the equilibrium zincate ion con-

* Corresponding author. Tel.: +1-212-854-4453; fax: +1-212-854-3054; E-mail: hyc1@columbia.edu

centration can cause large variations in the short-time behavior of zincate ion in the cell. A lower initial accumulation of zincate ion will lead to lower zincate ion concentration profiles throughout a discharge. When combined with the revision of the cathode specific interfacial area [5], which leads to zincate ion depletion, the zincate ion is expected to be totally consumed in a localized region of the cell to a larger extent.

The second goal of this study is the correction of the voltage fluctuations when the zincate ion concentration approaches zero in a localized region of the cell. The ternary to binary electrolyte transition is a unique area to be studied in the battery literature. The governing equations for such a transition are given in Podlaha and Cheh's model [1], but the actual simulation of such behavior has never been presented. The voltage fluctuations must be corrected because the model cannot be considered robust, and truly applicable to the high-rate discharge regime, until these inconsistencies are resolved. From the two objectives of this study, the physical effect of the zincate ion on the cell performance can be obtained. As in the previous revision study [5], the entire analysis is performed using a single, published AA-size test design [1–5].

2. Equilibrium zincate ion concentration

2.1. Dissolution–precipitation mechanism

A detailed overview of the Zn/MnO_2 cylindrical alkaline cell is given elsewhere [1]. A basic description is listed here. The Zn/MnO_2 system initially contains a porous Zn anode, a porous MnO_2 cathode, and a porous, inert separator. The cell is flooded with KOH electrolyte. The liquid phase is considered a concentrated ternary electrolyte because of the presence of the tetrahydroxozincate ion [8], $Zn(OH)_4^{2-}$, herein referred to as the zincate ion.

When the cell is discharged, zincate ion is formed when zinc is oxidized, which is stated as

$$Zn + 4OH^- \rightarrow Zn(OH)_4^{2-} + 2e^- \qquad (1)$$
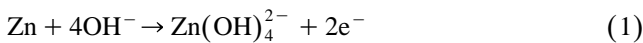
The zincate ion then precipitates to form solid zinc oxide by a homogeneous chemical reaction, described by

$$Zn(OH)_4^{2-} \rightarrow ZnO + H_2O + 2OH^- \qquad (2)$$
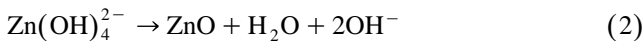
These two reactions are the zincate ion dissolution–precipitation mechanism. When discharging, zincate ion is produced in the anode and diffuses throughout the entire cell in the electrolyte phase. Solid zinc oxide is produced when the precipitation reaction occurs. In the Zn/MnO_2 model, the forward precipitation reaction proceeds when the zincate ion concentration is larger than the equilibrium zincate ion concentration given by this reaction. Dissolution of ZnO is not assumed to occur throughout a discharge.

2.2. Current model

The equilibrium zincate ion concentration refers to the equilibrium state of the homogeneous chemical precipitation reaction. Zincate ion is formed from solid zinc only by electrochemical reaction. Podlaha and Cheh's model [1] uses two different equilibrium expressions. The first expression is used to calculate the initial zincate ion concentration in the electrolyte phase. It is the same formulation used by Sunu [9], and Sunu and Bennion [10].

After the start of discharging, the current model switches to a different equilibrium zincate ion concentration expression, given by Isaacson et al. [11]. This expression gives a higher equilibrium concentration than Sunu's expression, and is given by

$$c_{1,eq} = \frac{c_2^2}{K_{eq}} \qquad (3)$$

where c_1 is the zincate ion concentration, $c_{1,eq}$ is the equilibrium zincate ion concentration, c_2 is the hydroxyl ion concentration, and K_{eq} is the equilibrium constant for the precipitation reaction, valued at 0.0232 mol/cm^3. The current model is contradictory because two expressions are used for $c_{1,eq}$. It will also be shown that Eq. (3) is inappropriate.

2.3. Model revision

Two literature sources [12,13] reveal that Eq. (3) actually models the solubility of zinc dihydroxide, $Zn(OH)_2$, in alkaline electrolyte and not the solubility of ZnO. Sunu's three-tier solubility expression [9] matches Kordesch's ZnO data [12] more closely than Eq. (3). Another equilibrium
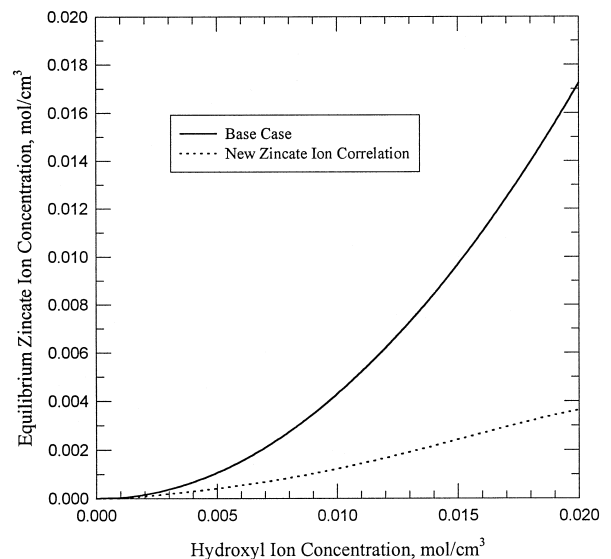

Fig. 1. Equilibrium zincate ion concentration expressions for the base case and the revised case.

expression is listed by Mao and White [14], but it is linear in KOH concentration and does not match the experimental data well over a large KOH concentration range.

The proposed revision of the equilibrium zincate ion concentration expression is a curve fit of Kordesch's zinc oxide solubility data [12]. The new expression is given as

$$c_{1,eq} = -9.25 \times 10^{-5} + 0.0974 c_2 - 3.11 c_2^2 + 951 c_2^3$$
$$- 2.86 \times 10^4 c_2^4 \tag{4}$$

This new form matches Kordesch's data better than Sunu's expression, and it is also easier to use because it is a single equation. Fig. 1 displays the current model expression from Eq. (3), and the revised expression from Eq. (4). The base case refers to Eq. (3). It is seen that the new expression is much lower than Eq. (3) for intermediate and large values of the hydroxyl ion concentration. This characteristic is important in modeling the ZnO precipitation rate.

3. Intrinsic precipitation rate

The anode formulation in Podlaha and Cheh's Zn/MnO_2 model [1] is adapted from Sunu's zinc electrode model [9,10]. Most of the model variables depend on the rate of the precipitation reaction, but the proportionality varies because of the reaction stoichiometry. A single reaction rate is presented based on Sunu's form, which is termed the intrinsic precipitation rate with the symbol R_p. Based on arguments by Podlaha [15], the Zn/MnO_2 model considers the precipitation reaction in the anode and the separator, but not in the cathode. In the anode, the intrinsic precipitation rate is given by $R_{p,a}$, and in the separator it is described by $R_{p,s}$. If $R_p > 0$ the precipitation reaction occurs, but if $R_p < 0$ the reverse reaction involving ZnO dissolution is not permitted. Only the forward precipitation reaction is allowed in the model. Neglecting ZnO dissolution is considered a good assumption for high-rate, primary discharges of the Zn/MnO_2 alkaline cell. R_p depends on a rate constant for the dissolution or precipitation reaction, a specific surface area, and a concentration driving force. The rate constant and the specific area are each different in the anode and separator.

3.1. Anode formulation

The intrinsic precipitation rate in the anode is given by

$$R_{p,a} = a_a k_s (c_1 - c_{1,eq}) \tag{5}$$

where a_a is the specific surface area for precipitation in the anode, and k_s is the dissolution or precipitation rate constant. The precipitation reaction occurs because of a concentration driving force with respect to $c_{1,eq}$. The active specific surface area for precipitation depends on the anode porosity. The dissolution or precipitation rate constant for the anode combines the initial mass transfer coefficient

of the aqueous potassium zincate salt, K_A^0, with the chemical rate constant for the dissolution or precipitation of ZnO, k_x. The form is [1]

$$k_s = \left[\frac{\ln\left(\dfrac{a_a}{a_a - a_m} \right)}{\dfrac{a_m}{a_a} K_A^0} + \frac{a_a}{(a_a - a_m) k_x} \right]^{-1} \tag{6}$$

where a_m is the specific active surface area for the electrochemical reaction of zinc, which is related to a_a and the volume fractions of solid species in the anode.

3.2. Separator formulation

The intrinsic precipitation rate in the separator is described by

$$R_{p,s} = a_s k_x (c_1 - c_{1,eq}) \tag{7}$$

where a_s is the specific surface area for precipitation in the separator, which depends on separator porosity [1]. The use of k_x means that only the chemical precipitation effects are included for the separator. The mass transfer analysis is not applied to the separator, although it is reasonable to expect that such an extension is applicable because the separator matrix should provide nucleation sites for precipitation [16]. The chemical rate constant for the dissolution or precipitation of ZnO, k_x, is a constant.

3.3. Relation of the intrinsic precipitation rate to the model governing equations

Many variables are influenced when zincate ion precipitates to form solid ZnO. Table 1 gives the source term dependence of the governing equation on the intrinsic precipitation rate for each of the relevant variables in the anode and separator. The governing equations are shown in Ref. [1]. The volume average velocity of the electrolyte is given by $\mathbf{v}$, and ϵ is the porosity.

3.4. Generalized concentration driving force

Let Δc_1 denote the zincate ion concentration driving force for ZnO precipitation. In Eqs. (5) and (7), the driving force is chosen as $(c_1 - c_{1,eq})$. This can be generalized to introduce supersaturation characteristics. Podlaha [15] ar-

Table 1
Relation of the intrinsic precipitation rate to the governing equations of the model

Variable	Proportionality in Anode	Proportionality in Separator
c_1	$-R_{p,a}$	$-R_{p,s}$
c_2	$2R_{p,a}$	$2R_{p,s}$
$\mathbf{v}$	$R_{p,a}$	$R_{p,s}$
ϵ	$-R_{p,a}$	$-R_{p,s}$

gued that data presented by Dirkse [17] suggest that the zincate ion concentration should be two to four times larger than the equilibrium value for ZnO precipitation to proceed.

Zhang and Cheh [18] expressed this mathematically by incorporating a supersaturation factor, ξ, into Δc_1. The generalized form is

$$\Delta c_1 = \left(c_1 - \xi c_{1,\text{eq}} \right) \tag{8}$$

where $\xi = 3.0$ was selected based on data from Briggs et al. [19]. This ξ value forces the zincate ion concentration to be three times larger than the equilibrium value before ZnO precipitation occurs. Zhang and Cheh did not present any zincate ion concentration profiles, nor was the effect of ξ examined. A goal of this study is to ascertain the effect of a different equilibrium expression on the zincate ion concentration, based on a model revision using more appropriate experimental data. Therefore, the supersaturation factor is not considered, so that $\xi = 1.0$ is used.

4. Additional equations

There are two other equations that are important for this study because of their dependence on c_1. They are the governing equation for Ohm's law in the electrolyte phase and the anode electrochemical kinetics expression.

Ohm's law in the electrolyte phase couples the ohmic resistances to the polarization of the cell, and it also contains the concentration overpotential terms. These concentration terms are crucial when c_1 approaches zero [5]. A general form for Ohm's law in the electrolyte phase is given as [3,9,14,15]

$$
\nabla \eta = \mathbf{i}_2 \left(\frac{1}{\kappa \epsilon^{1.5}} + \frac{1}{\sigma} \right) - \frac{\mathbf{I}}{\sigma}
$$
$$
+ \frac{1}{nF} \left(\frac{s_1}{\nu_{1\text{A}}} + \frac{nt_1}{z_1 \nu_{1\text{A}}} - \frac{s_0}{c_0} c_1 \right) \nabla \mu_\text{A}
$$
$$
+ \frac{1}{nF} \left(\frac{s_2}{\nu_{2\text{B}}} + \frac{nt_2}{z_2 \nu_{2\text{B}}} - \frac{s_0}{c_0} c_2 \right) \nabla \mu_\text{B} \tag{9}
$$

where η is the local overpotential, $\mathbf{i}_2$ is the superficial current density in the electrolyte phase, κ is the electrolyte conductivity, σ is the effective matrix conductivity, $\mathbf{I}$ is the cell current density vector, c_0 is the solvent concentration, s_i is the stoichiometric coefficient for species i in the arbitrary reference electrode reaction, $\nu_{1\text{A}}$ and $\nu_{2\text{B}}$ are the number of molecules of species i $(1 = \text{Zn(OH)}_4^{2-}, 2 = \text{OH}^-)$ that can dissociate completely from one molecule of salt A or B$(A = \text{K}_2\text{Zn(OH)}_4$, $B = \text{KOH})$, t_i is the transference number of species i defined with respect to the volume average velocity of the electrolyte, and z_i is the charge number for ionic species i. The respective electrochemical potentials for the potassium zincate and potassium hydroxide aqueous salts are given by μ_A and μ_B.

Ohm's law in the electrolyte phase is applied in each cell region [1].

The electrochemical potentials of the aqueous salts depend on the ionic concentrations through [20]

$$\mu_\text{A} = 3RT \ln \left(f_\text{A} c_1 a_\text{A}^\theta \right) \tag{10}$$

and

$$\mu_\text{B} = 2RT \ln \left(f_\text{B} c_2 a_\text{B}^\theta \right) \tag{11}$$

where T is the cell temperature, f_i is the mean molar activity coefficient of the electrolyte with aqueous salt i, and a_i^θ is a proportionality constant for aqueous salt i that expresses a secondary reference state. The mean molar activity coefficients depend on the ionic concentrations of the zincate ion and the hydroxyl ion. Therefore, Ohm's law in the electrolyte phase has a complicated, logarithmic dependence on the ionic concentrations.

Podlaha and Cheh [1] used a Butler–Volmer type expression for the electrochemical reaction rate in the anode, j_a, based on data from Bockris et al. [21]. The anodic transfer current is given by

$$
j_\text{a} = a_\text{m} i_0 \left[\left(\left(\frac{c_{1,\text{s}}}{c_{1,\text{ref}}} \right)^{0.06} \left(\frac{c_{2,\text{s}}}{c_{2,\text{ref}}} \right)^{2.59} \exp\left(\frac{\alpha_\text{a} F}{RT} \eta \right) \right. \right.
$$
$$
\left. \left. - \left(\frac{c_{1,\text{s}}}{c_{1,\text{ref}}} \right)^{0.94} \left(\frac{c_{2,\text{s}}}{c_{2,\text{ref}}} \right)^{-0.92} \exp\left(-\frac{\alpha_\text{c} F}{RT} \eta \right) \right] \tag{12}
$$

where i_0 is the exchange current density for the Zn oxidation reaction evaluated at a reference condition, $c_{i,\text{s}}$ is the surface concentration of species i [9,10], $c_{i,\text{ref}}$ is a reference concentration of species i, and α_a and α_c are the transfer coefficients for the electrochemical reaction. The dependence of j_a on the ionic concentrations is non-elementary and nonlinear.

5. Results

5.1. Overview

Two simulations are performed with a 1.0 A discharge rate with a 0.8 V cutoff voltage using an AA-size configuration that was used in previous work [1–5]. All model equations and parameter values are identical to those shown in Ref. [1]. The exception is the cathode specific area, a_c^0, which has been revised [5] with a new value of $a_\text{c}^0 = 6.03 \times 10^4$ cm^{-1}. The initial KOH concentration is 0.007 mol/cm^3. One simulation is performed using the base case equilibrium zincate ion concentration expression. This is referred to as the base case simulation. The other simulation uses the revised expression for the equilibrium zincate ion concentration. This is termed the revised case simulation. The discharge rate and cutoff voltage pairing conforms to the earlier work, and reflects primary operation in the high-rate discharge regime.

5.2. Cell voltage

Fig. 2 shows the cell voltage curves for the two cases. The revised case has a higher operating voltage for the entire discharge after the start of operation. The difference in operating voltage is roughly 30 mV for most of the discharge. The cell voltage begins fluctuating at an earlier time for the revised case than for the base case. This suggests that the zincate ion becomes depleted in a localized region of the cell at an earlier time for the revised case. The discharge time, t_d, for the base case is 1.150 h. The discharge time with the new zincate ion correlation is 1.211 h, which is a 5.31% increase with respect to the base case. The revised expression for the equilibrium zincate ion concentration leads to the prediction of better cell performance, but the voltage fluctuations need to be addressed.

5.3. Zincate ion concentration

Fig. 3 shows the zincate ion concentration profiles throughout the cell with the base case expression for $c_{1,eq}$. The anode is on the left side, the separator is the thin area marked off by the two dotted, vertical lines, and the cathode is on the right side. The concentration more than doubles its initial value at short times in the anode and separator, and then the concentration in these regions decreases throughout the rest of the discharge. This is an inconsistency because the concentration uniformly jumps to the higher value at short times, although there is very little penetration depth of the electrochemical reaction in the anode. It is reasonable if the concentration jump is localized instead to the anode/separator interface, because of the large transfer current that produces zincate ion at this location. At short times, there is a very large concen-
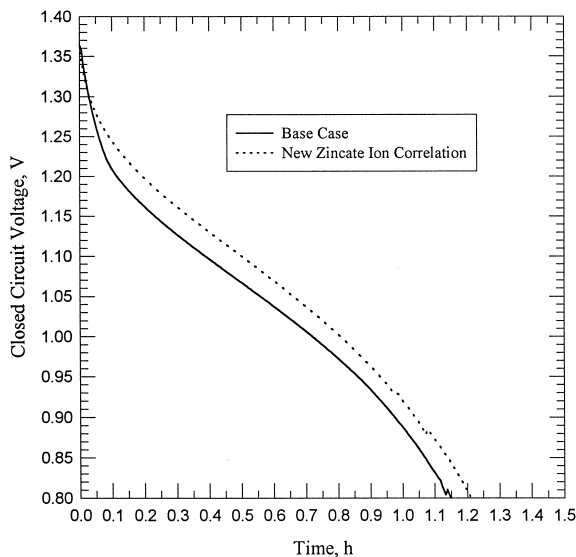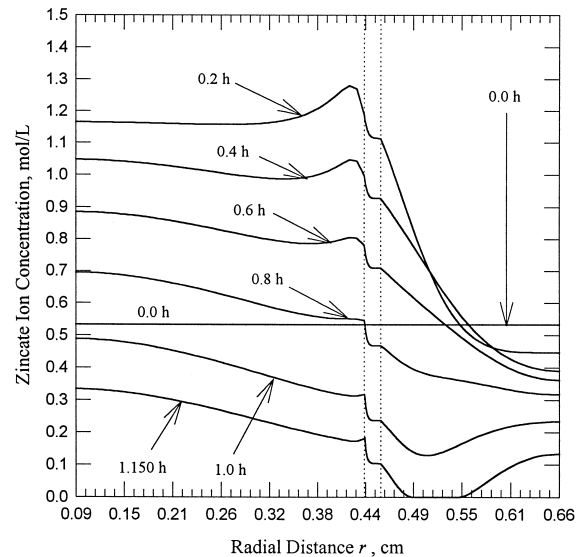

Fig. 3. Zincate ion concentration profiles in the entire cell for the base case equilibrium zincate ion concentration expression.

tration gradient in the cathode. The zincate ion is continuously depleted in the cathode. Near the end of the discharge, there is a localized region in the cathode that is totally depleted of the zincate ion. This is identified as the cause of the cell voltage fluctuations. Podlaha and Cheh [1] found migration forces to dominate the zincate ion flux in the cathode at longer times, which act to push zincate ion out of this region.

Fig. 4 gives the zincate ion concentration profiles throughout the cell with the revised expression for $c_{1,eq}$. There are major differences when this figure is compared to the base case profiles. The important change is that c_1 is much lower throughout the cell at all times after discharging begins. There is no concentration jump at short times,

Fig. 2. Cell voltage curves for the base case and the revised case equilibrium zincate ion concentration expressions.
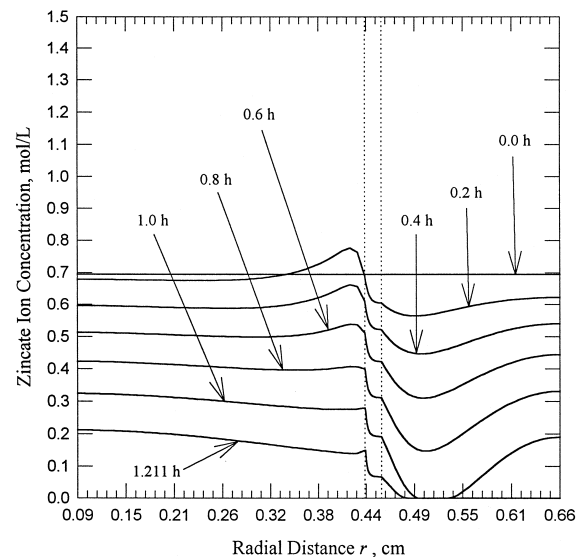

Fig. 4. Zincate ion concentration profiles in the entire cell for the revised equilibrium zincate ion concentration expression.

except for a slight accumulation near the anode/separator interface and this is a rational prediction. The zincate ion continuously decreases from its initial value throughout the discharge. The gradients in zincate ion concentration are reduced, especially in the cathode at short times. Near the end of the discharge, the cathode has become almost totally depleted of zincate ion. The lower overall zincate ion amount in the system leads to a more substantial exhaustion of the zincate ion. The zincate ion concentration first reaches zero at an earlier time for the revised case, which is consistent with the earlier appearance of the voltage fluctuations in Fig. 2.

In both Figs. 3 and 4, the point when the zincate ion reaches zero is termed the ternary to binary electrolyte transition, since there is still a large concentration of hydroxyl ion in the localized region where the zincate ion is depleted. Electrolytic current should flow without any drastic effects. This is supported by the very low value of the zincate ion transference number for this system [1]. As in Fig. 3 and the earlier revision study [5], the voltage fluctuations occur because of numerical difficulty in implementing the ternary to binary electrolyte transition. This problem is not discussed in the literature. Hauser and Newman [22] discussed related phenomena regarding supporting electrolytes, but the results cannot be applied to a complete battery model. Podlaha [15] did show a curve where c_1 reaches zero, but there was no mention of this characteristic. Mao and White [14] showed zincate ion concentration profiles that become close to zero. They discussed the case when hydroxyl ion appears to be depleted at a location where zincate ion is not totally depleted. They concluded that hydroxyl ion depletion is sufficient to cause cell failure.
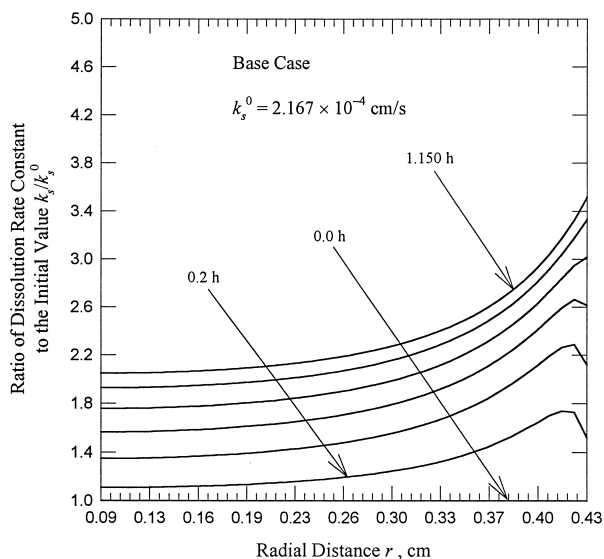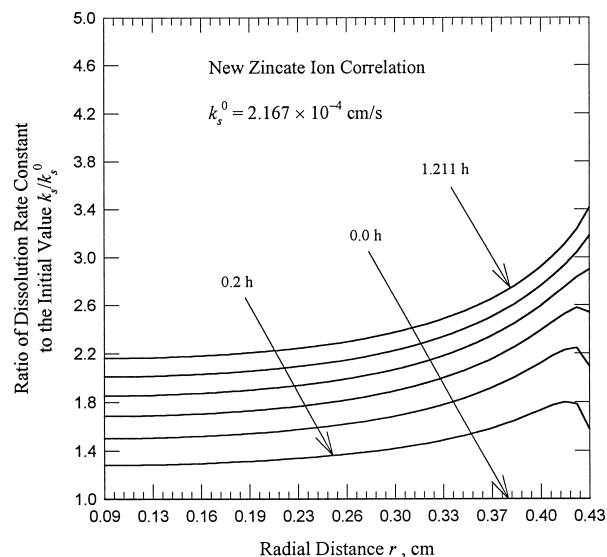

Fig. 6. Dissolution or precipitation rate constant in the anode for the revised equilibrium zincate ion concentration expression.

5.4. Intrinsic precipitation rate

The intrinsic precipitation rates in the anode and separator are analyzed to quantitatively demonstrate the large accumulation of zincate ion at short times for the base case, as well as the removal of this effect for the revised case. The lower zincate ion concentration profiles are explained if R_p is larger for the revised case.

The profiles for a_a and a_m in the anode are similar for both simulations. The specific surface area for the precipitation reaction in the anode, a_a, is roughly 50 cm^{-1} for both cases, with a minimum value of about 30 cm^{-1} and a maximum value of about 60 cm^{-1}. The effect of this change in a_a on $R_{p,a}$ is not expected to be large. The specific surface area for the electrochemical reaction in the anode, a_m, is roughly 40 cm^{-1} throughout the anode for both cases, with a minimum value of about 5 cm^{-1} near the anode/separator interface.

However, k_s increases throughout the anode for both cases. The initial value of k_s is the same for both cases. Figs. 5 and 6 show the k_s profiles in the anode for both simulations. This is the first time that k_s values from the model are reported. The k_s values rise uniformly in the anode to between two and three times the initial value by the end of the discharges. Although a_a and a_m do not change drastically on average, their combined effect on Eq. (6) is substantial. The rate constant is expected to have a large influence on $R_{p,a}$. The profiles for k_s are similar for the base case and the revised case simulations. For the revised case, k_s is larger for most of the anode except near the anode/separator interface, where the base case values slightly exceed the revised case values at longer times. The larger differences in k_s between the two simulations are observed in the anode interior.

The profiles of $R_{p,a}$ are analyzed on a smaller time scale in order to explain the short-time behavior of the

Fig. 5. Dissolution or precipitation rate constant in the anode for the base case equilibrium zincate ion concentration expression.
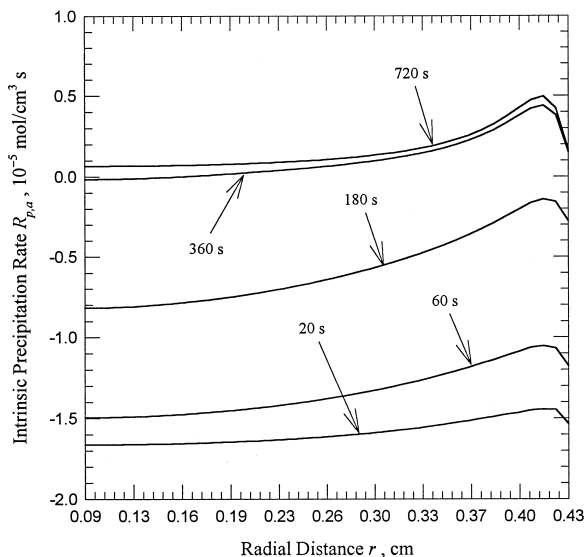
Fig. 7. Intrinsic precipitation rate in the anode for the base case equilibrium zincate ion concentration expression.

zincate ion. Figs. 7 and 8 display the short-time $R_{p,a}$ profiles in the anode for the base case and revised case simulations, respectively. At times less than 3 min, $R_{p,a} < 0$ in almost the entire anode for the base case. There is minimal calculated consumption of zincate ion, because when $R_p < 0$ no precipitation or dissolution is calculated. It is not until after 6 min that $R_{p,a} > 0$ for the entire anode. The electrochemical reaction rate in the anode is very large near the anode/separator interface. Zincate ion is produced by the oxidation of Zn, and with $R_{p,a} < 0$ this explains the large accumulation of zincate ion in the anode for the base case. Fig. 8 shows that $R_{p,a} > 0$ in the anode at all times after discharging begins for the simulation with the revised $c_{1,eq}$ expression. The model calculates immedi-
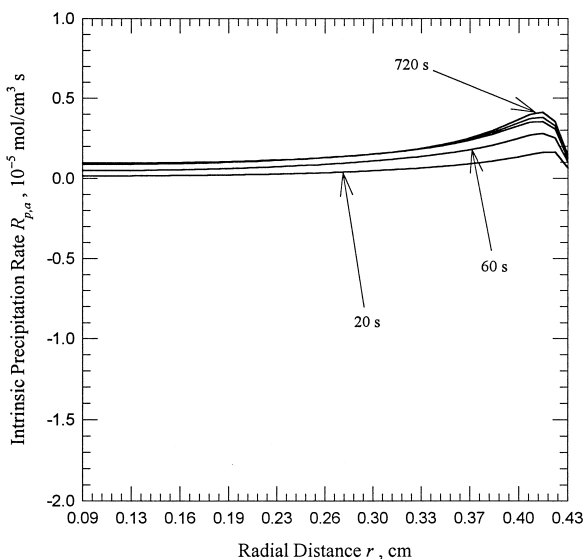
ate and continuous consumption of zincate ion in the anode. This explains why there is no net accumulation of zincate ion in the anode for the revised case.

The direction of R_p is determined by the sign of Δc_1, which is taken as $(c_1 - c_{1,eq})$. If $c_{1,eq} > c_1$, the precipitation reaction will not proceed, and accumulation of zincate ion results. If $c_1 > c_{1,eq}$, the forward precipitation reaction occurs and zincate ion is consumed. This demonstrates the effect of $c_{1,eq}$ on the c_1 profiles. A lower $c_{1,eq}$ expression results in lower zincate ion concentration profiles. The larger $c_{1,eq}$ expression permits an overprediction of zincate ion accumulation. Since the hydroxyl ion concentration decreases in the anode and separator, $c_{1,eq}$ decreases. The result is that R_p rises in time. This concept was described by Mao and White [14]. $R_{p,a}$ also rises because of the changes in k_s.

The profiles for a_s in the separator are close in value for both simulations. Throughout the discharges, a_s varies between $15–30$ cm^{-1}, with an initial value of 30 cm^{-1}. Thus, a_s is the same order of magnitude as a_a and a_m during operation. The value for k_x is 0.005 cm/s, which is about an order of magnitude larger than the k_s profiles. Figs. 9 and 10 present the profiles of $R_{p,s}$ in the separator at short times during the base case and revised case discharges, respectively. Qualitatively, they are similar to the $R_{p,a}$ profiles. For the base case, $R_{p,s} < 0$ for the first few minutes of the discharge, leading to zincate ion accumulation in the separator. For the revised case, $R_{p,s} > 0$ for all times during the discharge, so that zincate ion is consumed in the separator at all periods. Therefore, the short-time accumulation of zincate ion for the base case, as well as the elimination of this behavior with the revised case, are explained for both cell regions by analysis of the intrinsic precipitation rate. The major effect of $c_{1,eq}$ is on

Fig. 8. Intrinsic precipitation rate in the anode for the revised equilibrium zincate ion concentration expression.
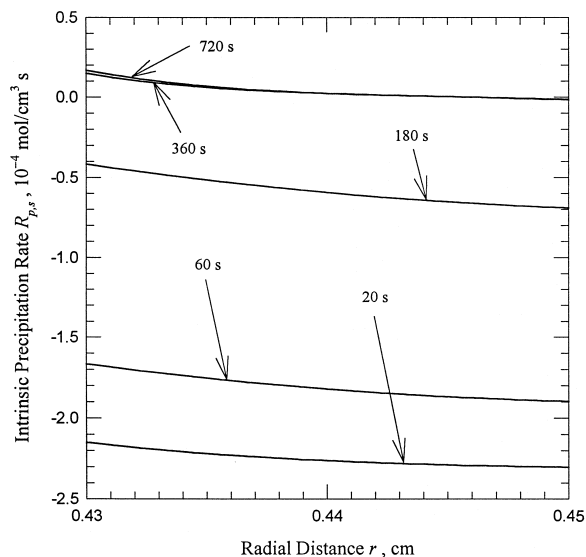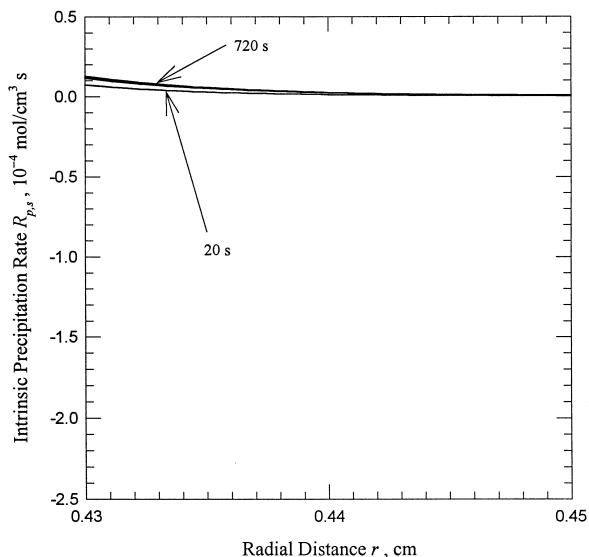

Fig. 9. Intrinsic precipitation rate in the separator for the base case equilibrium zincate ion concentration expression.

Fig. 10. Intrinsic precipitation rate in the separator for the revised equilibrium zincate ion concentration expression.

Fig. 12. Transfer current profiles in the entire cell for the revised equilibrium zincate ion concentration expression.

the sign of the intrinsic precipitation rate, from calculation of the quantity $(c_1 - c_{1,eq})$. In general, the $R_{p,s}$ values are about an order of magnitude larger than the $R_{p,a}$ values. This is due to the larger value of k_x, which may artificially overpredict the amount of ZnO precipitation that occurs in the separator.

5.5. Transfer current

The transfer current profiles in the entire cell for the base case and the revised case are shown in Figs. 11 and 12, respectively. There is no transfer current in the separator. The differences between the figures are not large, but they provide useful information. In the anode interior at
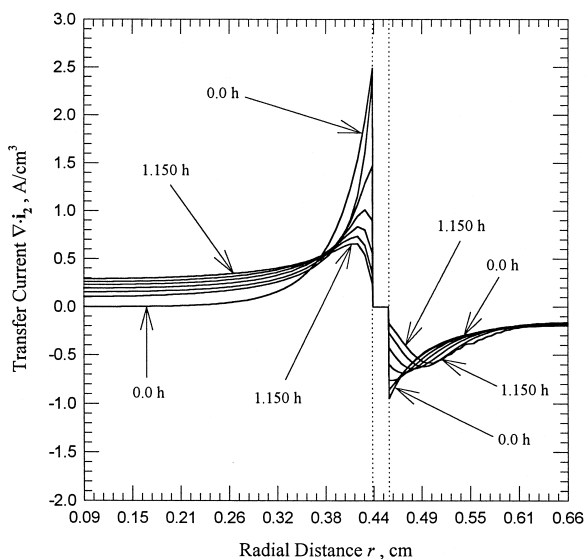

Fig. 11. Transfer current profiles in the entire cell for the base case equilibrium zincate ion concentration expression.
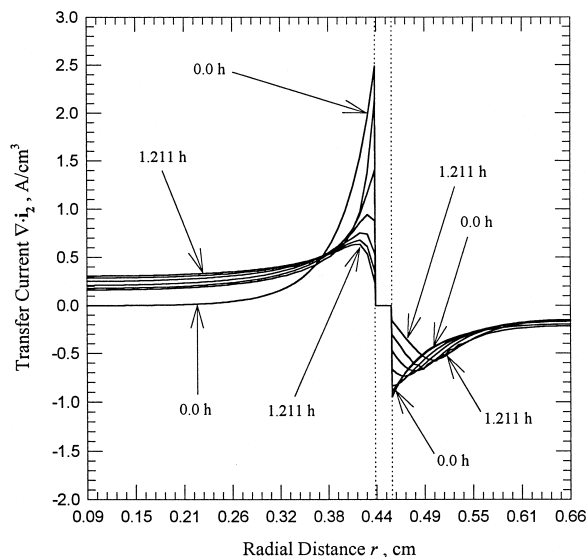
short times, the reaction rate is larger for the revised case. At longer times, the transfer current profiles in the anode are close for both cases, but the reaction rate near the anode/separator interface is lower for the revised case. The current distribution is slightly more uniform in the anode for the revised case.

The revised case possesses lower local overpotential values than the base case, for all times in the anode during the discharges. This is explained by the more uniform zincate ion and hydroxyl ion concentration profiles in the anode for the revised case. Lower gradients of c_1 and c_2 yield a lower gradient in η, as given by Ohm's law in the electrolyte phase. Thus, there is less polarization in the anode as the concentration profiles become more uniform. The revised c_1 profiles, in addition to the more uniform η profiles, contribute to more uniform current distribution profiles. The hydroxyl ion concentration is larger in the anode for the revised case because hydroxyl ion is produced in the precipitation reaction at short times in the anode and separator. Also, the hydroxyl ion concentration gradient is more uniform in the anode and separator, and this contributes to less concentration polarization in the anode. Since c_2 will be larger in the anode, and j_a depends on c_2 as shown in Eq. (12), j_a will increase as c_2 increases. This explains the larger and more uniform transfer current in the anode with less polarization, for the revised case.

Comparison of the revised case and the base case at different times shows that the anode polarization is consistently about 30 mV larger in magnitude for the base case. The higher operating voltage for the revised case is explained by the more benign overpotential profiles in the anode, which result from the more uniform ionic concentration profiles. A major conclusion is that the new equilib-

rium zincate ion concentration expression causes the simulated improvement in cell performance because of ionic concentration effects.

5.6. ZnO volume fraction

At short times in the discharges, the ZnO volume fraction values in the anode and separator are larger for the revised case. This observation is consistent with the intrinsic precipitation rate analysis that showed the precipitation reaction occurring at short times for the revised case, although the precipitation reaction is delayed for the base case. At longer times, the ZnO volume fractions are larger for the base case. This is because of the larger overall amount of zincate ion available for the precipitation reaction in the base case. The continuous depletion of zincate ion for the revised case leads to a slightly lower overall amount of precipitated ZnO.

6. Numerical remedies

The voltage fluctuations near the end of the discharges for the base case and the revised case are assumed to be caused by inconsistencies from switching the ternary form of Ohm's law in the electrolyte phase to the binary form, as a result of c_1 reaching zero in a localized section of the cell. The model is then solving two different forms of Ohm's law in the electrolyte phase at different parts of the cell. The reason that two different forms are used is because of the logarithmic singularity that occurs when c_1 approaches zero in the ternary form, shown in Eq. (9). A new form is used for the region where c_1 is zero. The ternary to binary electrolyte transition results in the model solution of Ohm's law in the electrolyte phase by neglecting the zincate ion concentration overpotential at the depleted location. This is considered to be the cause of the fluctuations in η, the local overpotential, and thus the cause of the cell voltage fluctuations. Because of the high sensitivity to η, the ternary to binary electrolyte transition should be smooth in such a way that η remains unchanged at the location and moment the zincate ion concentration reaches zero. This would require the possible alteration of any of the following quantities in an iteration scheme: $\mathbf{i}_2$, $\mathbf{I}$, and c_2. It is deemed nonphysical to iterate upon any of these quantities to ensure η remains unchanged upon the ternary to binary electrolyte transition. It should also be stated that Zhang and Cheh's [18] technique of setting $\mathbf{i}_2$ to zero, at the location where c_1 is zero, is not appropriate.

A smooth implementation of the ternary to binary electrolyte transition appears to be a difficult numerical problem. Therefore, it is desirable to try a simplified approach to assess the importance of the zincate ion in relation to the fluctuations, by showing that Ohm's law in the electrolyte phase is where they appear. The simplest method is to decouple c_1 from Ohm's law in the electrolyte phase.

This implies modeling the system as a pseudo-binary electrolyte, in that a material balance for c_1 is still included and the anode electrochemical kinetics are not changed, but Ohm's law in the electrolyte phase will reflect a binary KOH system. The general binary form is

$$\nabla \eta = \mathbf{i}_2 \left(\frac{1}{\kappa \epsilon^{1.5}} + \frac{1}{\sigma} \right) - \frac{\mathbf{I}}{\sigma}$$
$$+ \frac{1}{nF} \left(\frac{s_2}{\nu_{2B}} + \frac{nt_2}{z_2 \nu_{2B}} - \frac{s_0}{c_0} c_2 \right) \nabla \mu_B \qquad (13)$$

It is necessary to calculate f_B, the mean molar activity coefficient of the KOH electrolyte, based on a binary electrolyte correlation [1]. The form of κ is not changed because Sunu's correlation [9] is for a binary electrolyte and does not consider the effect of the zincate ion. Also, t_2 is not changed to its binary value because the effect is minimal due to the low value of t_1.

This formulation can be applied to different cell regions, while still considering the remainder of the cell to have a ternary electrolyte. The main point is that the voltage fluctuations will not occur because the binary form is calculated instead, from the beginning of discharge, at the cell locations where c_1 is known to approach zero. The binary form must be used in at least the cathode because this is where the localized region of zero zincate ion concentration develops.

Simulations are performed with the new $c_{1,eq}$ expression, using the binary form of Ohm's law in the electrolyte phase in different cell regions. Three possibilities are considered: binary form in the cathode only, binary form in the cathode and separator, and binary form in the entire cell. The cell voltage curves for these three cases are shown in Fig. 13. All three curves are plotted, although they appear as a single curve because the discharge characteristics are almost identical. There are no voltage fluctua-
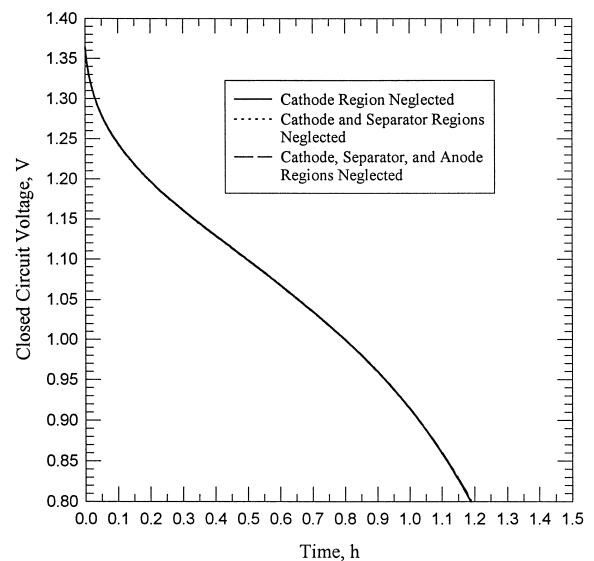
Fig. 13. Cell voltage curves for the three numerical remedy simulations.

Table 2
Summary of the numerical remedy simulations

Scheme	t_d (h)	t_d increase, above base case (%)	Does $c_1 = 0$ in cathode?	Cell voltage fluctuations?
Base case	1.150	–	Yes	Yes
Revised case	1.211	5.31	Yes	Yes
Numerical remedy: cathode	1.189	3.38	No	No
Numerical remedy: cathode and separator	1.190	3.48	Yes	No
Numerical remedy: entire cell	1.192	3.64	Yes	No

tions in any of these discharges. It is concluded that the ternary to binary electrolyte transition, in the context of the ternary form of Ohm's law in the electrolyte phase, causes the voltage fluctuations. The simplified numerical remedies successfully remove these fluctuations.

A summary of the three numerical remedies is provided in Table 2. All three simulations give discharge time improvements with respect to the base case design, but they all have shorter discharge times than the revised case. The zincate ion does not become fully depleted in any cell location for the numerical remedy applied to the cathode only. But the two other simulations experience the depletion of zincate ion in the cathode, although the cell voltage fluctuations are removed. The main effect of the binary form of Ohm's law in the electrolyte phase is derived when it is applied to the cathode. The incremental improvements in discharge time for the other two simulations are small compared to the result when the binary form is applied to just the cathode.

The numerical remedies are not physically realistic because they weaken the assumption of a concentrated ternary electrolyte. The Zn/MnO_2 model [1] applies concentrated ternary electrolyte theory mainly through Ohm's law in the electrolyte phase. Altering this fundamental equation relegates the model to the status of a pseudo-binary electrolyte. Perhaps there is a rational justification to model the system as a true binary electrolyte, with the complete neglect of the zincate ion.

7. Conclusions

Revising the equilibrium zincate ion concentration expression provides information about the zincate ion concentration effect on the cell performance. Lower values of $c_{1,eq}$ lead to lower values in the zincate ion concentration profiles, based on the analysis of the ZnO precipitation behavior. The lower and more uniform c_1 profiles are responsible for the simulated improvement in cell performance. The cell voltage fluctuations are determined to occur because of the ternary to binary electrolyte transition. These fluctuations are successfully removed by the

incorporation of a pseudo-binary form of Ohm's law in the electrolyte phase. The effect of the zincate ion concentration on the cell performance is discernible, but it is not major, except in the case of the adverse voltage fluctuations. The numerical remedies are not acceptable because they negate the assumption of concentrated ternary electrolyte theory. It seems reasonable to explore whether a binary electrolyte model of the Zn/MnO_2 cell is justified. The binary electrolyte model would neglect the formation of zincate ion with the assumption of direct ZnO formation in the anode. It may also serve as a useful model benchmark.

8. List of symbols

a_a	specific active surface area for the precipitation reaction in the anode, cm^{-1}
a_m	specific active surface area for the electrochemcial reaction of Zn, cm^{-1}
a_s	specific active surface area for the precipitation reaction in the separator, cm^{-1}
a_c^0	initial specific interfacial area in the cathode, cm^{-1}
a_i^θ	proportionality constant for aqueous salt i and the solvent that expresses a secondary reference state, cm^3/mol
c_i	concentration of species i, mol/cm^3
$c_{i,s}$	concentration of species i on the active Zn surface, mol/cm^3
$c_{i,ref}$	reference concentration of species i, mol/cm^3
c_1	zincate ion concentration, mol/cm^3
$c_{1,eq}$	equilibrium zincate ion concentration, mol/cm^3
Δc_1	concentration driving force for the ZnO precipitation reaction, mol/cm^3
f_i	mean molar activity coefficient of the electrolyte with aqueous salt i
F	Faraday's constant, 96,487 C/mol
$\mathbf{I}$	cell current density vector, A/cm^2
i_0	anode exchange current density at a reference condition, A/cm^2
$\mathbf{i}_2$	superficial current density in the solution phase, A/cm^2
j_a	transfer current in the anode, A/cm^3
k_s	dissolution or precipitation rate constant for the ZnO precipitation reaction in the anode, cm/s
k_x	chemical rate constant for the dissolution or precipitation of ZnO, cm/s
K_A^0	initial mass transfer coefficient of the aqueous potassium zincate salt, cm/s
K_{eq}	equilibrium constant in Eq. (3), mol/cm^3
n	number of electrons transferred in the reference electrode reaction
R	universal gas constant, 8.3143 J/mol K
R_p	intrinsic precipitation rate, mol/cm^3 s
$R_{p,a}$	intrinsic precipitation rate in the anode, mol/cm^3 s

$R_{p,s}$ intrinsic precipitation rate in the separator, mol/cm^3 s

s_i stoichiometric coefficient of species i in the reference electrode reaction

t_d discharge time to reach the cutoff voltage, h

t_i transference number of species i with respect to the volume average velocity

T cell temperature, K

$\mathbf{v}$ volume average velocity in the electrolyte, cm/s

z_i charge number of species i

Greek

α_a anodic transfer coefficient for the anode electrochemical reaction

α_c cathodic transfer coefficient for the anode electrochemical reaction

ϵ porosity

η local overpotential, V

κ electrolyte conductivity, Ω^{-1} cm^{-1}

μ_i electrochemical potential of aqueous salt i, J/mol

ν_{ij} number of ions of species i contained in one molecule of salt j

ξ supersaturation factor

σ effective matrix conductivity, Ω^{-1} cm^{-1}

Main subscripts

A   potassium zincate
B   potassium hydroxide
0   solvent (water)
1   zincate ion
2   hydroxyl ion

Superscripts

0   initial condition

References

[1] E.J. Podlaha, H.Y. Cheh, J. Electrochem. Soc 141 (1994) 15.
[2] E.J. Podlaha, H.Y. Cheh, J. Electrochem. Soc. 141 (1994) 28.
[3] J.J. Kriegsmann, H.Y. Cheh, J. Power Sources 77 (1999) 127.
[4] J.J. Kriegsmann, H.Y. Cheh, J. Power Sources 79 (1999) 262.
[5] J.J. Kriegsmann, H.Y. Cheh, J. Power Sources 84 (1999) 114.
[6] M. Doyle, T.F. Fuller, J. Newman, Electrochim. Acta 39 (1994) 2073.
[7] B. Paxton, J. Newman, J. Electrochem. Soc. 143 (1996) 1287.
[8] C. Debiemme-Chouvy, J. Vedel, M.-C. Bellissent-Funel, R. Cortes, J. Electrochem. Soc. 142 (1995) 1359.
[9] W. G. Sunu, PhD Thesis, University of California, Los Angeles, CA, 1978.
[10] W.G. Sunu, D.N. Bennion, J. Electrochem. Soc. 127 (1980) 2007.
[11] M.J. Isaacson, F.R. McLarnon, E.J. Cairns, J. Electrochem. Soc. 137 (1990) 2014.
[12] K.V. Kordesch, in: K.V. Kordesch (Ed.), Batteries, Manganese Dioxide (Fig. 62), Marcel Dekker, New York, Vol. 1, 1974, p. 348.
[13] S.U. Falk, A.J. Salkind, Alkaline Storage Batteries (Fig. 8.8), Wiley, New York, 1969, p. 586.
[14] Z. Mao, R.E. White, J. Electrochem. Soc. 139 (1992) 1105.
[15] E.J. Podlaha, PhD Thesis, Columbia University, New York, 1992.
[16] O. Söhnel, J. Garside, Precipitation: Basic Principles and Industrial Applications, Butterworth-Heinemann, Boston, MA, 1992.
[17] T.P. Dirkse, J. Electrochem. Soc. 128 (1981) 1412.
[18] Y. Zhang, H.Y. Cheh, J. Electrochem. Soc. 146 (1999) 850.
[19] A.G. Briggs, N.A. Hampson, A. Marshall, J. Chem. Soc., Faraday Trans. 2 (70) (1974) 1978.
[20] J.S. Newman, Electrochemical Systems, 2nd ed., Prentice-Hall, Englewood Cliffs, NJ, 1991.
[21] J.O'M. Bockris, Z. Nagy, A. Damjanovic, J. Electrochem. Soc. 119 (1972) 285.
[22] A.K. Hauser, J. Newman, J. Electrochem. Soc. 136 (1989) 3319.